Strong charge and spin fluctuations in $La_2O_3Fe_2Se_2$

Guangxi Jin,[1,2] Yilin Wang,[3] Xi Dai,[3] Xinguo Ren,[1,2] and Lixin He[1,2]

[1]*Key Laboratory of Quantum Information, University of Science and Technology of China, Hefei 230026, China*

[2]*Synergetic Innovation Center of Quantum Information and Quantum Physics, University of Science and Technology of China, Hefei 230026, China*

[3]*Beijing National Laboratory for Condensed Matter Physics and Institute of Physics, Chinese Academy of Sciences, Beijing 100190, China*

(Received 30 November 2015; revised manuscript received 13 July 2016; published 25 August 2016)

The electronic structure and magnetic properties of the strongly correlated material $La_2O_3Fe_2Se_2$ are studied by using both the density-functional theory plus U (DFT + U) method and the DFT plus Gutzwiller (DFT + G) variational method. The ground-state magnetic structure of this material obtained with DFT + U is consistent with recent experiments with an appropriate U parameter, but its band gap is significantly overestimated by DFT + U, even with a small Hubbard U value. In contrast, the DFT + G method yields a band gap of 0.1–0.2 eV, in excellent agreement with experiment. Detailed analysis shows that the electronic and magnetic properties of $La_2O_3Fe_2Se_2$ are strongly affected by charge and spin fluctuations which are missing in the DFT + U method.

DOI: 10.1103/PhysRevB.94.075150

I. INTRODUCTION

Because of their close relationship with the Fe-based high-T_c superconductor, there has been revived interest in iron oxychalcogenides, $R_2O_3T_2X_2$ (R = rare-earth element, T = transition-metal element, X = S or Se), which have similar crystal structures [1,2]. One example is $La_2O_3Fe_2Se_2$ (LOFS), which was first explored by Mayer *et al.* [3] and considered to be a strongly correlated material composed of the transition-metal ion Fe^{2+}. Analogous to its oxychalcogenides relatives, LOFS was determined to be a semiconductor by experiment and claimed to be a Mott insulator [2].

The crystal structure of LOFS with space-group $I4/mmm$ (No. 139) is shown in Fig. 1, and the corresponding Wyckoff positions are listed in Table I. It is composed of alternating layered units of $[La_2O_2]^{2+}$ and $[Fe_2OSe_2]^{2-}$, stacking along the c axis. The layered sheets of $[La_2O_2]^{2+}$, formed by edge-sharing La_4O tetrahedra, expand along the a-b plane. The $[Fe_2OSe_2]^{2-}$ layers consist of face-sharing FeO_2Se_4 octahedra where the Fe atom is surrounded by two axial oxygen atoms and four equatorial selenium atoms, forming a tilted Fe-centered octahedron with the D_{2h} point symmetry. Viewed along the c axis, the Fe atoms in the $[Fe_2OSe_2]^{2-}$ layer form a checkerboard lattice, and the Fe-Fe interactions are mediated by Fe-O-Fe and Fe-Se-Fe bonds.

Despite the considerable research in the past, there are still some mysteries about this material to be understood. First, the magnetic structure of LOFS was found to be antiferromagnetic (AFM) below the critical temperature of $T_N \sim 90$ K. However, two possible magnetic ground states have been proposed by experiments. The first model (model I) was proposed in Ref. [2]. Within this model, the AFM ground state is described by the propagation vector $\mathbf{k} = (0.5,0,0.5)$, and the Fe atoms form a spin-frustrated magnetic structure, which aligns ferromagnetically (FM) along the a axis and antiferromagnetically along the b axis [2,4]. An interesting aspect of this magnetic structure is that it lacks inversion symmetry, which may further break the inversion symmetry of the crystal, resulting in ferroelectricity by the exchange-striction effect as possible magnetic ferroelectrics [5,6]. The second model (model II) is a noncollinear AFM model, which is composed of two magnetic sublattices with propagation vectors $\mathbf{k}_1 = (0.5,0,0.5)$ and $\mathbf{k}_2 = (0,0.5,0.5)$, respectively. This magnetic structure was first proposed by Fuwa *et al.* [7] for $Nd_2O_3Fe_2Se_2$ and was identified as the magnetic structure for LOFS by recent experiments [8,9]. Within this model, the spins align in parallel in each sublattice and perpendicular between different sublattices. In contrast with model I, the magnetic structure of model II still possesses the inversion symmetry.

Second, the magnitude of the local magnetic moment measured by different experiments scatters significantly, ranging from 2.62 to 3.50 μ_B [2,4,8,9]. Thus information from reliable first-principles calculations will be helpful to clarify the situation.

Third, LOFS was determined to be a semiconductor by electrical resistivity measurement with a small band gap of 0.17–0.19 eV [1,4,10]. However, the band gaps obtained by the DFT + U method, even for very small Hubbard U parameters, are significantly larger than the experimental values. This suggests that the Hartree-Fock-type treatment of electron correlations, which neglects the multiplet effects, might not be sufficient for this system.

In this paper, we first identify the ground-state magnetic structure of LOFS via first-principles calculations. We calculated the total energies of different magnetic structures using density-functional theory (DFT) with an on-site Coulomb interaction correction (DFT + U), including the two experimentally proposed magnetic structure models. Our results suggest that the model II spin configuration is the ground-state magnetic structure of LOFS. However, the DFT + U method greatly overestimates the band gap of LOFS [11]. In order to correctly describe the electronic structure of LOFS [1,10], we further calculated the electronic and magnetic properties of this compound by the DFT plus Gutzwiller (DFT + G) method. With appropriate U, J parameters, the obtained DFT + G band gap is approximately 0.1–0.2 eV, in excellent agreement with experiment. The local magnetic moment obtained by DFT + G is about 3.0 μ_B, falling within the range of experimental results, but is somewhat smaller than the DFT + U values, which are approximately 3.4–3.6 μ_B. Detailed analysis shows that there are strong charge and spin fluctuations in this system,

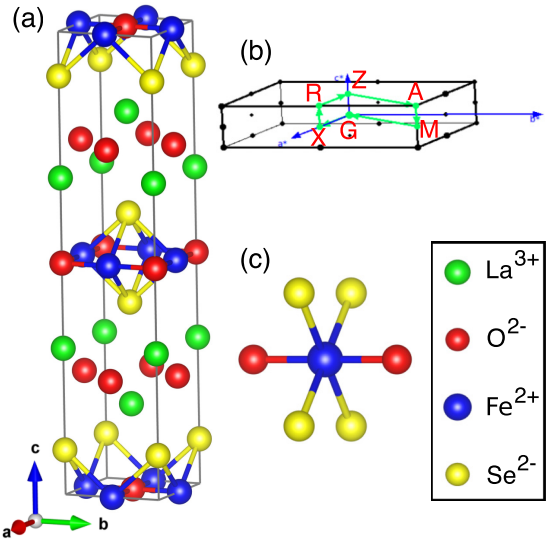

FIG. 1. (a) Crystal structure of LOFS where green, red, blue, and yellow balls represent La^{3+}, O^{2-}, Fe^{2+}, and Se^{2-}, respectively; (b) Symmetry points in the Brillouin zone; (c) FeO_2Se_4 octahedra where the Fe atom is surrounded by two axial oxide atoms and four equatorial selenide atoms, forming a tilted Fe-centered octahedron with the D_{2h} point symmetry.

which are responsible for the significant reduction of the band gap and the magnetic moments. The strong charge and spin-fluctuation effects to the electronic structures of various iron pnictides have been studied previously [12–18], however most of these materials are metals with bad-metal behavior, whereas LOFS is a semiconductor [1,4].

The rest of the paper is organized as follows. In Sec. II, the methods used in our calculations are described. In Sec. III A, we determine the ground-state magnetic structure of LOFS by comparing the total energies of various spin configurations using the DFT + U method. In Sec. III B, we study its band structure using the DFT + G method. A summary of our work is given in Sec. IV.

II. COMPUTATIONAL DETAILS

A. DFT + U

We perform first-principles calculations based on DFT within the spin-polarized generalized gradient approximation (GGA) and Perdew-Burke-Ernzerhof functional [19], implemented in the Vienna *ab initio* simulations package [20,21]. The projector-augmented-wave pseudopotentials with a 500-eV plane-wave cutoff are used. To account for the correlation effect of Fe atoms, we apply on-site Coulomb interaction U as is performed in the DFT + U scheme [22]. The total energies are converged to 10^{-8} eV.

TABLE I. Internal atomic coordinates (IACs) of nonequivalent Wyckoff positions (WPs) with the different occupied atoms (OAs) in the LOFS crystal where the oxygen atoms occupy two nonequivalent WPs, which are denoted as O(1) and O(2) below.

WP	OA	IAC
4*e*	La	$(\frac{1}{2},\frac{1}{2},0.18407)$
4*d*	O(1)	$(\frac{1}{2},0,\frac{1}{4})$
4*c*	Fe	$(\frac{1}{2},0,0)$
2*b*	O(2)	$(\frac{1}{2},\frac{1}{2},0)$
4*e*	Se	(0,0,0.09618)

B. DFT + G

LOFS is a strongly correlated system, whose band structure understandably cannot be well described by single-particle mean-field approximations, such as DFT + U. As mentioned above and detailed below, the band gaps obtained from DFT + U calculations are too big. To correct this, we resort to the DFT + G variational method [23,24], which can treat the multiplet effects more accurately [16]. The DFT + G method starts with the following many-body Hamiltonian:

$$\begin{aligned}\hat{H} &= \hat{H}_{TB} + \hat{H}_{\text{int}} + \hat{H}_{dc} \\ &= \hat{H}_{TB} + \sum_i \hat{H}_{i,\text{atom}} - \sum_i \hat{H}_{i,dc}. \end{aligned} \tag{1}$$

The first term in Eq. (1) is a d-p tight-binding (TB) Hamiltonian constructed from a non-spin-polarized GGA band structure, projected to the d-p manifold of maximally localized Wannier functions [25–28]. This term apparently describes the hopping of electrons. Since the Wannier functions contain not only the localized 3d orbitals of Fe atoms, but also the extended 2p orbitals of O atoms and 4p orbitals of Se atoms, the model takes account of the hybridization of p-d orbitals [13]. Using the Wannier functions, the TB term can be written more explicitly as

$$\begin{aligned}\hat{H}_{TB} = &\sum_{\substack{i,j\\ m_1,m_2\\ \sigma}} t_{i,j}^{m_1\sigma,m_2\sigma}\, \hat{d}^{\dagger}_{im_1\sigma}\hat{d}_{jm_2\sigma} \\ &+ \sum_{\substack{i,j\\ m_1,m_2\\ \sigma}} t_{i,j}^{m_1\sigma,m_2\sigma}\, \hat{p}^{\dagger}_{im_1\sigma}\hat{p}_{jm_2\sigma} \\ &+ \sum_{\substack{i,j\\ m_1,m_2\\ \sigma}} t_{i,j}^{m_1\sigma,m_2\sigma}\, \hat{d}^{\dagger}_{im_1\sigma}\hat{p}_{jm_2\sigma} \\ &+ \sum_{\substack{i,j\\ m_1,m_2\\ \sigma}} t_{i,j}^{m_1\sigma,m_2\sigma}\, \hat{p}^{\dagger}_{im_1\sigma}\hat{d}_{jm_2\sigma} \end{aligned} \tag{2}$$

where the operator $\hat{d}^{\dagger}_{im\sigma}$ ($\hat{d}_{im\sigma}$) creates (annihilates) a 3d electron of a Fe atom on site i with orbital m and spin σ. Likewise, $\hat{p}^{\dagger}_{im\sigma}$ ($\hat{p}_{im\sigma}$) creates (annihilates) a p electron of O and Se atoms. As depicted in Fig. 2, the TB band structures are in excellent agreement with the original band structures obtained from GGA calculations.

The second term in Eq. (1) is a rotationally invariant Coulomb interaction Hamiltonian describing the strong on-site electron-electron interactions within the 3d orbitals of Fe atoms. We assume the spherical symmetry of local environment of the Fe atom and use a full interaction tensor as

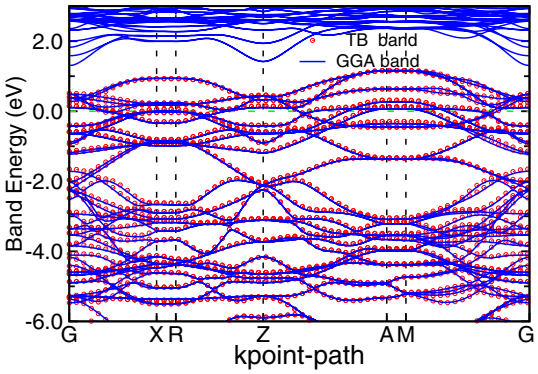

FIG. 2. Comparison of the non-spin-polarized GGA band structures and the down-folded tight-binding band structures.

$U_{m_1\sigma,m_2\sigma',m_3\sigma',m_4\sigma}$. For the detailed definition of the U tensor, we follow the method described in Ref. [29]. Within the complex spherical harmonics basis, the second term of the Hamiltonian in Eq. (1) can be explicitly expressed as [30]

$$\hat{H}_{i,\text{atom}} = \sum_{\substack{m_1,m_2,m_3,m_4 \\ \sigma,\sigma'}} U_{m_1\sigma,m_2\sigma',m_3\sigma',m_4\sigma} \times \hat{d}^{\dagger}_{m_1\sigma}\hat{d}^{\dagger}_{m_2\sigma'}\hat{d}_{m_3\sigma'}\hat{d}_{m_4\sigma}, \quad (3)$$

where the U tensor satisfies the condition,

$$U_{m_1\sigma,m_2\sigma',m_3\sigma',m_4\sigma} = \delta_{m_1+m_2,m_3+m_4}\sum_k c_k^{m_1,m_4}c_k^{m_2,m_3}F^k. \quad (4)$$

Here, m_1, m_2, m_3, and m_4 are the orbital indices, σ,σ' denote the spin states, $c_k^{m_1,m_4}$ are the Gaunt coefficients, and F^k are the Slater integrals. For the d shell, $k = 0,2,4$, and hence the full U tensor can be specified by the parameters F^0, F^2, and F^4. According to Wang *et al.* [29], $F^4/F^2 = 0.625$ is an approximation with good accuracy for the d shell [31] and hence is also adopted in this paper. The intraorbital Coulomb interaction and Hund's rule coupling are set to be $U = F^0 + \frac{4}{49}F^2 + \frac{4}{49}F^4$ and $J = \frac{5}{98}(F^2 + F^4)$, respectively. Therefore, given the parameter values of either F^0, F^2 or U, J, we can construct the full interaction U tensor.

The last term of Eq. (1) is a double-counting (DC) term in order to subtract the correlation effect which has been partially included in DFT calculations. The DC term is not uniquely defined, and here we adopted the choice used in Ref. [32] where it can be expressed as

$$\hat{H}_{dc} = \sum_\sigma U_{dc}^\sigma \hat{n}_d^\sigma,$$
$$U_{dc}^\sigma = U\left(n_d - \frac{1}{2}\right) - J\left(n_d^\sigma - 1\right)/2, \quad (5)$$
$$n_d^\sigma = \sum_m \langle\Psi_G|\hat{d}^{\dagger}_{m\sigma}\hat{d}_{m\sigma}|\Psi_G\rangle.$$

When treating the nonmagnetic DFT band structure as the starting point of DFT + G calculations [16], the average occupation number of $3d$ electrons per Fe is calculated to be $\bar{n}_d = 6.828$.

The Gutzwiller trial wave-function $|\Psi_G\rangle$ is constructed by applying a projection operator $\hat{P}$ on the uncorrelated wave-function $|\Psi_0\rangle$ from DFT calculations,

$$|\Psi_G\rangle = \hat{P}|\Psi_0\rangle, \quad (6)$$

with

$$\hat{P} = \prod_{\mathbf{R}}\hat{P}_{\mathbf{R}} = \prod_{\mathbf{R}}\sum_{\Gamma,\Gamma'}\lambda(\mathbf{R})_{\Gamma\Gamma'}|\Gamma,\mathbf{R}\rangle\langle\Gamma',\mathbf{R}|, \quad (7)$$

where $|\Gamma,\mathbf{R}\rangle$ are the eigenstates of the on-site Hamiltonian $\hat{H}_{i,\text{atom}}$ for site $\mathbf{R}$ and $\lambda(\mathbf{R})_{\Gamma\Gamma'}$ are the Gutzwiller variational parameters to be determined by minimizing the total energy of the ground-state $|\Psi_G\rangle$ through the variational method [23,24]. More details of this method can be found in Refs. [24,33].

III. RESULTS AND DISCUSSION

In this section, we first study the magnetic ground state of LOFS using the DFT + U method. The most stable magnetic configuration coming out from our DFT + U calculations agrees with the one proposed by Fuwa and co-workers [7]. However, as mentioned above, the DFT + U method significantly overestimates the band gap of LOFS. We then study the band structure of LOFS using the DFT + G method.

A. Results from DFT + U

In order to identify the magnetic structure of the ground state, we performed a series of DFT + U total energy calculations for different magnetic configurations. In LOFS, each unit cell contains two $[Fe_2OSe_2]^{2-}$ layers along the c axis. Atomic positions of the second $[Fe_2OSe_2]^{2-}$ layer are shifted by (0.5, 0.5, 0.5) of the lattice vectors relative to the first layer. Possible magnetic configurations in each layer are shown in Fig. 3. The magnetic structures in a unit cell are then the combinations of the magnetic configurations of the two layers. For example the configuration $[(b) + (a)]$ means the first layer takes configuration (b), whereas the second layer takes configuration (a). This notational system is similar to that used by Zhu *et al.* [1] and Zhao *et al.* [11].

We calculated the total energies of seven magnetic structures, including (1) FM$[(a) + (a)]$, (2) AFM1$[(c) + (c)]$, (3) AFM2$[(b) + (a)]$, (4) AFM3$[(g) + (g)]$, (5) AFM4$[(d) + (f)]$, (6) AFM5$[(e) + (e)]$, and (7) AFM6$[(d) + (d)]$. In the AFM3 configuration, the spins in each $[Fe_2OSe_2]^{2-}$ layer form a double stripe AFM structure along the a axis [2], which is different from the structure used in Refs. [1,11]. AFM3 is actually the experimental magnetic structure model I proposed by Free and Evans [2], whereas the AFM6 configuration corresponds to the experimental magnetic model II, within the collinear approximation. Such an approximation was previously adopted for $Sr_2F_2Fe_2OS_2$ in Ref. [11] because the magnetic-anisotropy energies are rather small compared to the energy differences between different configurations.

Experimentally it was found that the spins form AFM along the c axis. We calculate the total energy of spin configurations with propagation vectors (1/2,0,1/2) and (1/2,0,0) for the experimental magnetic model I (AFM3) using a $2 \times 1 \times 2$ supercell. We found that the energy difference between the AFM spin configuration along the c axis with magnetic propagation

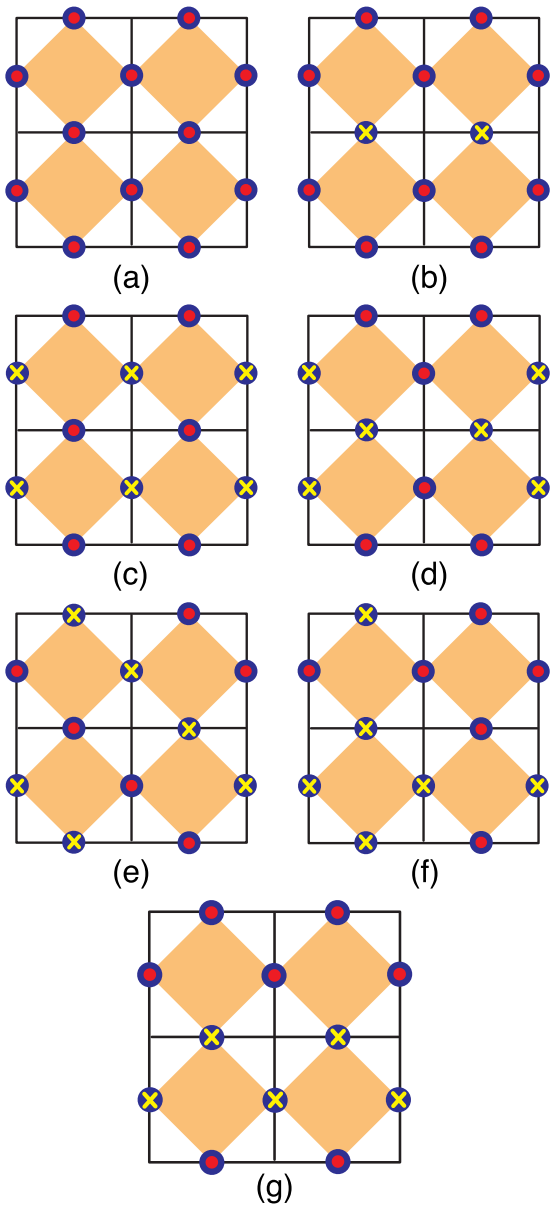

FIG. 3. (a)–(g) The magnetic structures of one layer of Fe atoms on the crystalline ab plane. Only the Fe atoms are shown in the figures, which is indicated by large blue circles; and the small red circle and yellow cross represent up- and down-spin orientations, respectively.

vector $\mathbf{k} = (0.5,0,0.5)$ and the ferromagnetic configuration along the c axis with propagation vector $\mathbf{k} = (0.5,0,0)$ is only about 0.1 meV in a $2 \times 1 \times 2$ sueprcell. Therefore, in the following studies, we ignore the antiferromagnetic configuration between the unit cells along the c axis and focus on the magnetic structure on the ab plane. To accommodate all seven magnetic structures, we use a $2 \times 2 \times 1$ supercell. The corresponding Monkhorst k mesh is set to $8 \times 8 \times 4$.

The calculated energies for different magnetic configurations are listed in Table II for various effective Coulomb $U_{\text{eff}} = U\text{-}J$, where U and J are the Coulomb and Hund's exchange interactions, respectively. One can see that, for all U_{eff}, the total energy of AFM6 is significantly lower than that of AFM3. The magnetic ground state of LOFS is AFM6

TABLE II. Relative energy ΔE (meV/unit cell) of different magnetic configurations and various parameter U_{eff} (in eV) with the reference energy of FM where the crystal structure was constrained at $I4/mmm$ space-group symmetry.

U_{eff}	FM	AFM1	AFM2	AFM3	AFM4	AFM5	AFM6
0	0	159.65	15.67	−120.09	−40.61	−10.04	−128.78
1.5	0	−237.42	−52.06	−237.12	−236.51	−341.42	−394.25
3.0	0	−220.76	−49.52	−194.86	−194.88	−273.04	−303.11
4.5	0	−184.12	−42.42	−148.38	−148.49	−201.93	−219.38
6.0	0	−601.95	−141.93	−441.21	−441.51	−576.26	−615.93
7.5	0	−485.69	−116.85	−321.79	−321.98	−398.46	−419.15

for $U_{\text{eff}} < 6.0$ eV. These results are consistent with previous DFT + U calculations for $Sr_2F_2Fe_2OS_2$ [11]. We therefore conclude that the experimental magnetic structure model II should be the ground-state magnetic structure in LOFS. We note however that, in Ref. [1], the ground state of LOFS was determined to be AFM6 for $U_{\text{eff}} = 0$, 1.5, and 3.0 eV but changed to AFM1 at $U_{\text{eff}} = 4.5$ eV. We also observe such a transition but at much larger $U_{\text{eff}} = 7.5$ eV.

For comparison, we also calculated the total energies of different magnetic configurations for $Pr_2O_3Fe_2Se_2$, which has the similar crystal structure as LOFS [34]. We found that its magnetic ground state is also AFM6 within the DFT + U approximation for U_{eff} less than 6.0 eV, the same as that of LOFS [1]. These results suggest that the model II magnetic structure should be the common character for the oxychalcogenide materials $R_2O_3Fe_2Se_2$.

After determining the ground-state magnetic structure, we calculate the magnetic moments of LOFS in the AFM6 configuration for different values of U_{eff}. The results are listed in Table III. The calculated magnetic moments of the Fe ions for different U_{eff} values are around 3.2 μ_B–3.7 μ_B, which are in agreement with the experimental result 3.50 μ_B, obtained by McCabe *et al.* [9].

To study the electronic structure of LOFS, we calculated the band structure and density of states by using the DFT + U method for the AFM6 spin configuration using different Coulomb $U_{\text{eff}} = 0$–6.0 eV. The typical band structures of LOFS with $U_{\text{eff}} = 1.5$ eV are shown in Fig. 4(a). Even for a small Coulomb $U_{\text{eff}} = 1.5$ eV, the band gap is as large as 1.12 eV, which is significantly larger than the energy gap of $E_g \sim 0.17$–0.19 eV, extracted from the electrical resistivity measurement [1,10]. The calculated band gaps as a function of U are shown in Fig. 4(b). For $U_{\text{eff}} = 0$, the system is metallic. For $U_{\text{eff}} > 0$, there is a nearly linear dependence of the band gap upon the U_{eff} value as can be seen from Fig. 4(b). For a reasonable $U_{\text{eff}} = 4.5$ eV, the calculated band gap is approximately 2.0 eV, which is about one order of magnitude larger than the experimental value. To check

TABLE III. Magnetic moment (magmom) of LOFS, calculated by the DFT + U method under the AFM6 magnetic configuration with different U_{eff}'s.

U_{eff} (eV)	0	1.5	3.0	4.5	6.0	7.5
Magmom (μ_B)	3.2	3.4	3.5	3.6	3.6	3.7

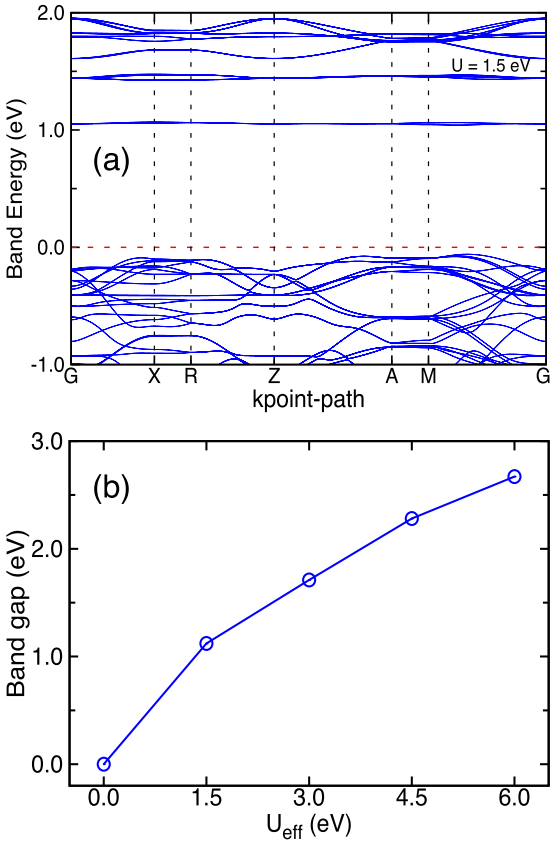

FIG. 4. (a) Band structure of LOFS calculated by the DFT + U method under the ground-state magnetic structure AFM6 and U_{eff} = 1.5 eV. The Fermi energy has been set to 0 eV. (b) Relation between the band gap of LOFS and U_{eff} calculated by the DFT + U method under the ground-state magnetic structure.

the spin-orbital coupling (SOC) effects on the band gaps of LOFS, we calculate the band structures of LOFS under the noncollinear magnetic configuration proposed by Ref. [9] for different U_{eff}'s with SOC interaction. The results are nearly the same with those without SOC. The results suggest that the correlation effects are not accounted for adequately by the DFT + U method and more advanced methods are needed to describe the electronic structure of LOFS.

B. Results from DFT + G

To correctly describe the electronic structure of LOFS, we perform DFT + G calculations under the magnetic structures AFM1, AFM3, AFM5, and AFM6. The relative energies of these magnetic structures are listed in Table IV for the typical values of $U = 6.0$ eV, $J = 0.25U$. As shown in the table, the

TABLE IV. Relative energy ΔE (meV/unit cell) of four major magnetic configurations with $U = 6.0$ eV, $J = 0.25U$, and the energy of AFM1 as the reference energy where the crystal structure was constrained at $I4/mmm$ space-group symmetry.

Configuration	AFM1	AFM3	AFM5	AFM6
ΔE	0.0	−237.5	−266.2	−400.0

TABLE V. The band gaps of LOFS, calculated by DFT + G method, under the AFM6 magnetic configuration for different Hubbard U and Hund's J parameters.

U (eV)	3.0	4.0	5.0	6.0	7.0
$J = 0.10U$	0.0	0.0	0.0	0.0	0.0
$0.15U$	0.0	0.0	0.0	0.0	0.061
$0.20U$	0.0	0.0	0.0	0.063	0.137
$0.25U$	0.0	0.0	0.0	0.121	0.203
$0.30U$	0.0	0.0	0.0	0.008	0.075

magnetic configuration AFM6 [8,9] has much lower energy than other configurations, especially AFM3 [2,4]. We therefore focus on AFM6 in the following discussions and perform calculations with a series of Hubbard $U = 3.0$–7.0 eV and Hund's exchange $J = 0.1$–$0.3U$.

The calculated band gaps for different Hubbard U and Hund's J parameters are listed in Table V. When U and J are small, LOFS is a metal. However, when further increasing U and J, LOFS becomes an insulator. The DFT + G calculated band gap is approximately 0.121 eV for $U = 6.0$ eV and $J = 0.25U$, which is in excellent agreement with the value obtained by the electric resistivity measurement [1,10]. This is in stark contrast with those obtained from DFT and DFT + U calculations. For example, DFT + U gives a very large band gap (approximately 2.28 eV) with $U_{\text{eff}} = 4.5$ eV, whereas DFT gives a metal for LOFS. These results clearly demonstrate that the multiplet effects, which are missing in the DFT + U methods but captured in the DFT + G method, are crucial for a correct description of the electronic structure of LOFS.

We also calculate the magnetic moments of Fe atoms using the Gutzwiller wave functions for different U and J parameters, and the results were listed in Table VI. The magnetic moments of Fe atoms are varying from 1.51 μ_B with $U = 3.0$ eV and $J = 0.1U$ to 3.09 μ_B with $U = 7.0$ eV and $J = 0.25U$. The magnetic moment is 3.08 μ_B with $U = 6.0$ eV and $J = 0.25U$ between the experimental results of Refs. [2,8], which are somehow smaller than those obtained from DFT + U calculations. The magnetic moments increase as the U and J parameters increase [16,18] but almost saturates for $U > 5$ and $J > 1$ eV.

The differences between the DFT + U and the DFT + G methods are that the DFT + G methods correctly take account of the multiplet effects resulting from the charge and spin fluctuation, whereas in the DFT + U methods only a single atomic configuration is considered. To understand

TABLE VI. The magnetic moments (unit μ_B) of the Fe atoms in LOFS, calculated by the DFT + G method under the AFM6 magnetic configuration with different on-site Hubbard U and Hund's J parameters.

U (eV)	3.0	4.0	5.0	6.0	7.0
$J = 0.10U$	1.51	1.68	2.40	2.88	2.98
$0.15U$	2.01	2.82	2.96	3.04	3.07
$0.20U$	2.75	2.92	3.03	3.07	3.09
$0.25U$	2.83	2.97	3.05	3.08	3.09
$0.30U$	2.91	3.00	3.05	3.08	3.09

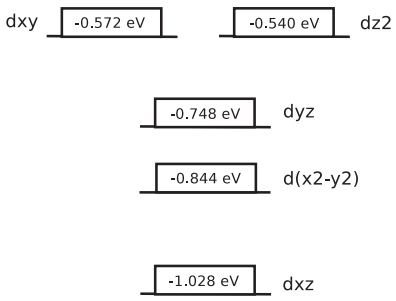

FIG. 5. Energy levels of Fe 3d states under crystal-field splitting.

the results, we further analyzed the Gutzwiller wave functions. We calculated the probability of the atomic multiplets $|I\rangle$ of Fe atoms using the Gutzwiller wave functions as $P_I = \langle G|I\rangle\langle I|G\rangle$. To display the atomic configuration more explicitly, the crystal-field splitting of a Fe atom is shown in Fig. 5. As we see the five Fe 3d orbitals are very close in energy near the Fermi level. It is expected that the charge fluctuation is strong in this system. The ten major atomic configurations with relatively large populations are shown in Fig. 6(a), and corresponding populations are shown in Fig. 6(b) for $U = 6.0$ eV and $J = 0.25U$.

First we look at the electron occupation numbers of these atomic configurations. The atomic configuration cf1 has occupation number $n = 5$ (yellow) and has the population $P(n = 5) = 0.015$. Configurations cf2 and cf3 have occupation number 6 (red), and their total population $P(n = 6) = 0.247$. Configurations cf4, cf5, cf6, cf7, and cf8 have occupation number 7 (blue) and total population $P(n = 7) = 0.4438$, and configurations cf9 and cf10 have occupation number 8 (green) with total population $P(n = 8) = 0.0826$. These results suggest that there are strong charge fluctuations on the Fe ions. In the DFT + U scheme, when adding a new electron into the system, it is forced to occupy one particular orbital and leads to very high energy. However, if charge fluctuations are allowed, the electron may partially occupy different configurations, resulting in much lower energy. Therefore, although the local interaction in this material is quite strong leading to Mott insulator behavior, the charge and spin fluctuation are still strong for such a multiorbital system, which reduces the single-particle gap from the value obtained by Hartree-Fock-type approximation (i.e., DFT + U) to about 0.1–0.2 eV.

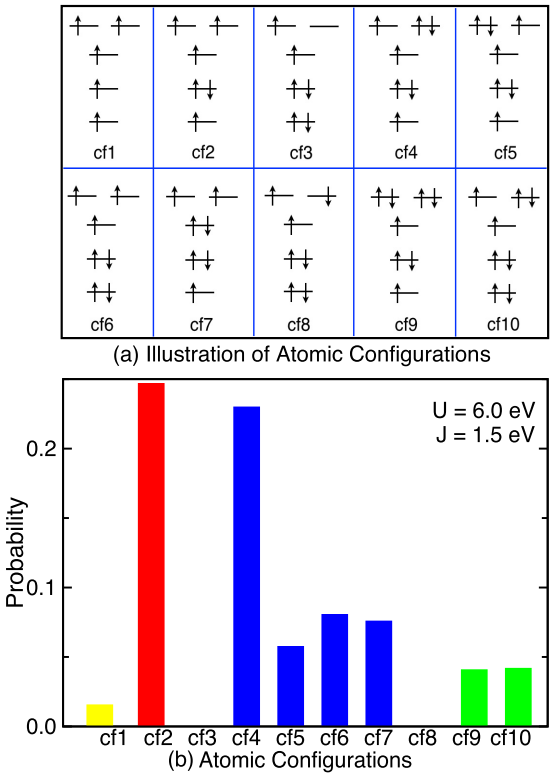

FIG. 6. (a) Illustration of the main atomic configurations with relatively large probability; (b) probability of the atomic configurations $|I\rangle$ in the Gutzwiller wave function $|G\rangle$, calculated with $U = 6.0$ eV and $J = 0.25U$ under the ground-state magnetic structure. Here, the atomic configurations with occupation numbers 5–8 are represented by histograms with the colors yellow, red, blue, and green, respectively.

Besides the charge fluctuation, there are also strong spin fluctuations on the Fe atoms. Configurations cf3, cf8, cf9, and cf10 have total spin $S = 2$. The total population of these configurations is $P(S = 2) = 0.0827$. Configurations cf4, cf5, cf6, and cf7 have total spin $S = 3$, and the their total population is $P(S = 3) = 0.4438$. Configuration cf2 has $S = 4$ and $P(S = 4) = 0.247$, and cf1 has $S = 5$ with $P(S = 5) = 0.015$. The most populated spin states in the DFT + G calculations are $S = 3$, which is smaller than the formal magnetic state $S = 4$ in the DFT + U calculations. As a result, the DFT + G calculated magnetic moments of Fe ions are smaller than those calculated by the DFT + U methods.

We note that Giovannetti *et al.* [35] and Freelon *et al.* [36] have studied the Mott insulator transition in LOFS using DFT + dynamical mean-field theory methods. However, both works focus on the high-temperature paramagnetic phase of LOFS, whereas in this paper, we study the low-temperature antiferromagnetic phase of LOFS. In contrast to the p-d model used in this paper, only d orbitals were considered in the previous works [35,36], and therefore the Mott insulator transition occurs at smaller U and J parameters.

IV. SUMMARY

We have studied the electronic structure and magnetic properties of the strongly correlated material $La_2O_3Fe_2Se_2$ using both DFT + U and DFT + G methods. The ground-state magnetic configurations obtained from DFT + U calculations with the appropriate parameter U_{eff} are in agreement with most recent experiments [8,9]. However, DFT + U calculations greatly overestimate the band gap of the material. We then investigate the electronic structure using the DFT + G method, and the results show $La_2O_3Fe_2Se_2$ is a narrow gap semiconductor, in excellent agreement with experiments. We show there are strong charge and spin fluctuations on the Fe atoms that greatly reduce the band gap from the DFT + U value.

ACKNOWLEDGMENTS

L.H. acknowledges support from Chinese National Science Foundation Grant No. 11374275. G.J. acknowledges valuable discussions with Hongwei Wang and Hong Jiang.

[1] J.-X. Zhu, R. Yu, H. Wang, L. L. Zhao, M. D. Jones, J. Dai, E. Abrahams, E. Morosan, M. Fang, and Q. Si, Phys. Rev. Lett. **104**, 216405 (2010).

[2] D. G. Free and J. S. O. Evans, Phys. Rev. B **81**, 214433 (2010).

[3] J. M. Mayer, L. F. Schneemeyer, T. Siegrist, J. V. Waszczak, and B. V. Dover, Angew. Chem., Int. Ed. Engl. **31**, 1645 (1992).

[4] S. Landsgesell, K. Prokeš, T. Hansen, and M. Frontzek, Acta Mater. **66**, 232 (2014).

[5] M. Fiebig, J. Phys. D: Appl. Phys. **38**, R123 (2005).

[6] S.-W. Cheong and M. Mostovoy, Nat. Mater. **6**, 13 (2007).

[7] Y. Fuwa, T. Endo, M. Wakeshima, Y. Hinatsu, and K. Ohoyama, J. Am. Chem. Soc. **132**, 18020 (2010).

[8] M. Günther, S. Kamusella, R. Sarkar, T. Goltz, H. Luetkens, G. Pascua, S.-H. Do, K.-Y. Choi, H. D. Zhou, C. G. F. Blum *et al.*, Phys. Rev. B **90**, 184408 (2014).

[9] E. E. McCabe, C. Stock, E. E. Rodriguez, A. S. Wills, J. W. Taylor, and J. S. O. Evans, Phys. Rev. B **89**, 100402(R) (2014).

[10] H. Lei, E. S. Bozin, A. Llobet, V. Ivanovski, V. Koteski, J. Belosevic-Cavor, B. Cekic, and C. Petrovic, Phys. Rev. B **86**, 125122 (2012).

[11] L. L. Zhao, S. Wu, J. K. Wang, J. P. Hodges, C. Broholm, and E. Morosan, Phys. Rev. B **87**, 020406(R) (2013).

[12] I. I. Mazin, M. D. Johannes, L. Boeri, K. Koepernik, and D. J. Singh, Phys. Rev. B **78**, 085104 (2008).

[13] M. Aichhorn, L. Pourovskii, V. Vildosola, M. Ferrero, O. Parcollet, T. Miyake, A. Georges, and S. Biermann, Phys. Rev. B **80**, 085101 (2009).

[14] M. Yi, D. H. Lu, J. G. Analytis, J.-H. Chu, S.-K. Mo, R.-H. He, M. Hashimoto, R. G. Moore, I. I. Mazin, D. J. Singh *et al.*, Phys. Rev. B **80**, 174510 (2009).

[15] T. Yildirim, Phys. Rev. Lett. **102**, 037003 (2009).

[16] T. Schickling, F. Gebhard, J. Bünemann, L. Boeri, O. K. Andersen, and W. Weber, Phys. Rev. Lett. **108**, 036406 (2012).

[17] L. Ortenzi, H. Gretarsson, S. Kasahara, Y. Matsuda, T. Shibauchi, K. D. Finkelstein, W. Wu, S. R. Julian, Y.-J. Kim, I. I. Mazin *et al.*, Phys. Rev. Lett. **114**, 047001 (2015).

[18] Z. P. Yin, K. Haule, and G. Kotliar, Nat. Phys. **7**, 294 (2011).

[19] J. P. Perdew, K. Burke, and M. Ernzerhof, Phys. Rev. Lett. **77**, 3865 (1996).

[20] G. Kresse and J. Hafner, Phys. Rev. B **47**, 558 (1993).

[21] G. Kresse and J. Furthmüller, Phys. Rev. B **54**, 11169 (1996).

[22] V. I. Anisimov, J. Zaanen, and O. K. Andersen, Phys. Rev. B **44**, 943 (1991).

[23] J. Bünemann, W. Weber, and F. Gebhard, Phys. Rev. B **57**, 6896 (1998).

[24] X. Y. Deng, L. Wang, X. Dai, and Z. Fang, Phys. Rev. B **79**, 075114 (2009).

[25] N. Marzari and D. Vanderbilt, Phys. Rev. B **56**, 12847 (1997).

[26] I. Souza, N. Marzari, and D. Vanderbilt, Phys. Rev. B **65**, 035109 (2001).

[27] N. Marzari, A. A. Mostofi, J. R. Yates, I. Souza, and D. Vanderbilt, Rev. Mod. Phys. **84**, 1419 (2012).

[28] A. A. Mostofi, J. R. Yates, Y.-S. Lee, I. Souza, D. Vanderbilt, and N. Marzari, Comput. Phys. Commun. **178**, 685 (2008).

[29] Y. Wang, Z. Wang, Z. Fang, and X. Dai, Phys. Rev. B **91**, 125139 (2015).

[30] A. Georges, L. de' Medici, and J. Mravlje, Annu. Rev. Condens. Matter Phys. **4**, 137 (2013).

[31] F. M. F. de Groot, J. C. Fuggle, B. T. Thole, and G. A. Sawatzky, Phys. Rev. B **42**, 5459 (1990).

[32] A. I. Liechtenstein, V. I. Anisimov, and J. Zaanen, Phys. Rev. B **52**, R5467 (1995).

[33] N. Lanatà, H. U. R. Strand, X. Dai, and B. Hellsing, Phys. Rev. B **85**, 035133 (2012).

[34] N. Ni, S. Jia, Q. Huang, E. Climent-Pascual, and R. J. Cava, Phys. Rev. B **83**, 224403 (2011).

[35] G. Giovannetti, L. de' Medici, M. Aichhorn, and M. Capone, Phys. Rev. B **91**, 085124 (2015).

[36] B. Freelon, Y. H. Liu, J.-L. Chen, L. Craco, M. S. Laad, S. Leoni, J. Chen, L. Tao, H. Wang, R. Flauca *et al.*, Phys. Rev. B **92**, 155139 (2015).